Electroactive Hydrophilic Polylactide Surface by Covalent Modification with Tetraaniline

ARTICLE *in* MACROMOLECULES · JANUARY 2012

Impact Factor: 5.8 · DOI: 10.1021/ma202508h

3 AUTHORS:

Baolin Guo
Xi'an Jiaotong University
41 PUBLICATIONS **653** CITATIONS
SEE PROFILE

Anna Finne-Wistrand
KTH Royal Institute of Technology
86 PUBLICATIONS **1,394** CITATIONS
SEE PROFILE

Ann-Christine Albertsson
KTH Royal Institute of Technology
419 PUBLICATIONS **11,377** CITATIONS
SEE PROFILE

Macromolecules

Article

pubs.acs.org/Macromolecules

Electroactive Hydrophilic Polylactide Surface by Covalent Modification with Tetraaniline

Baolin Guo, Anna Finne-Wistrand, and Ann-Christine Albertsson*

Department of Fibre and Polymer Technology, School of Chemical Science and Engineering, KTH Royal Institute of Technology, SE-100 44 Stockholm, Sweden

Supporting Information

ABSTRACT: Covalent surface functionalization is presented as a versatile tool to increase the hydrophilicity and to introduce the electroactivity of polyester films. Acrylic acid and maleic anhydride were photografted onto a polylactide (PLA) surface with a "grafting from" method to increase the surface wettability, and the subsequent coupling of conductive aniline oligomer was used to introduce electroactivity to the PLA surface. The photopolymerization of maleic anhydride and acrylic acid and the coupling of aniline tetramer (AT) were characterized by FT-IR, UV, and TGA. The surface morphology of the PLA surface before and after modification was examined by scanning electron microscopy (SEM) and atomic force microscopy (AFM). A medium hydrophilic surface of PLA was achieved by surface modification with maleic anhydride, acrylic acid, and AT. An electrically conductive surface was obtained after grafting with AT, and the conductivity increased with increasing AT content on the surface. The hydrophilic and electroactive surface of polyesters while retaining their bulk properties offers new possibilities in biomedical applications, such as bone, cartilage, neural, and cardiovascular tissue engineering.

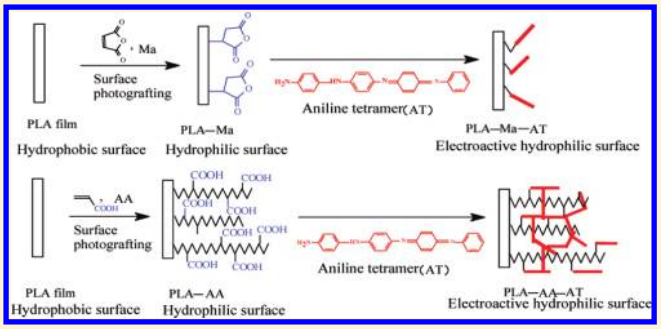

INTRODUCTION

The performance of polymeric materials depends greatly on the surface properties of the biomaterials because most biological reactions occur between a polymeric implant and the host tissue.[1−3] The development of biomaterials for tissue regeneration applications requires the construction of a suitable surface that can induce a specific cellular response and regulate the formation of new tissue. The most widely used biomaterials in tissue engineering are polyesters such as polylactide (PLA), polycaprolactone (PCL), etc., because of their excellent biocompatibility, degradability, and mechanical properties.[4−6] However, the hydrophilicity of PLA is not appropriate for cell attachment on its surface; the PLA surface lacks chemically modifiable side-chain groups, and PLA is a biologically inert polymeric biomaterial that is not able to induce cell adhesion and tissue formation.[7,8] To improve the host−implant interaction of biomaterials, various modifications of PLA have been studied,[8−10] such as copolymerization with other functional and hydrophilic monomers[11−13] or blending of PLA with other materials.[14,15] However, copolymerization and blending changes the bulk properties of PLA, and this is considered to be a drawback in many applications. Therefore, surface modification of the PLA has been the subject of attention. Among the techniques employed for surface modification of biodegradable polymers, photografting is a useful tool with the advantages of low cost of operation, mild reaction conditions, and a permanent alteration of the surface chemistry.[16,17] Photografting employs a much lower energy than γ or electron beam irradiation, and this reduces the risk of possible degradation of the polymer. Poly(acrylic acid) (PAA) has been covalently grafted onto the surface of degradable biomaterials including PLA and PCL by photografting.[18,19] PLA has a much more hydrophilic surface after grafting with AA or maleic anhydride, and the rate of degradation of PLA was enhanced as a result of the hydrophilic surface.[20,21] More importantly, the surface with functional groups could be used for the further covalent immobilization of bioactive molecules, such as gelatin, heparin, and nerve growth factor or vascular endothelium growth factor,[2] which could enhance cell adhesion and further regulate the cell behavior.

Conducting polymers such as polyaniline and polypyrrole have been shown to regulate the behavior of a series of cells (neural, cardiac, fibroblast, and endothelial cells) by electrical stimulation, including cell adhesion, spreading, proliferation, differentiation, and DNA synthesis.[22−24] To take advantage of conducting polymers, polypyrrole was coated onto electrospun poly(lactic-*co*-glycolic acid) nanofibers[25] and PLA and PCL nanofibers[26] by in situ solution polymerization of pyrrole. However, the interaction between the polypyrrole and substrate is weak due to the noncovalent deposition. Another severe

Received: November 15, 2011
Revised: December 16, 2011
Published: December 28, 2011

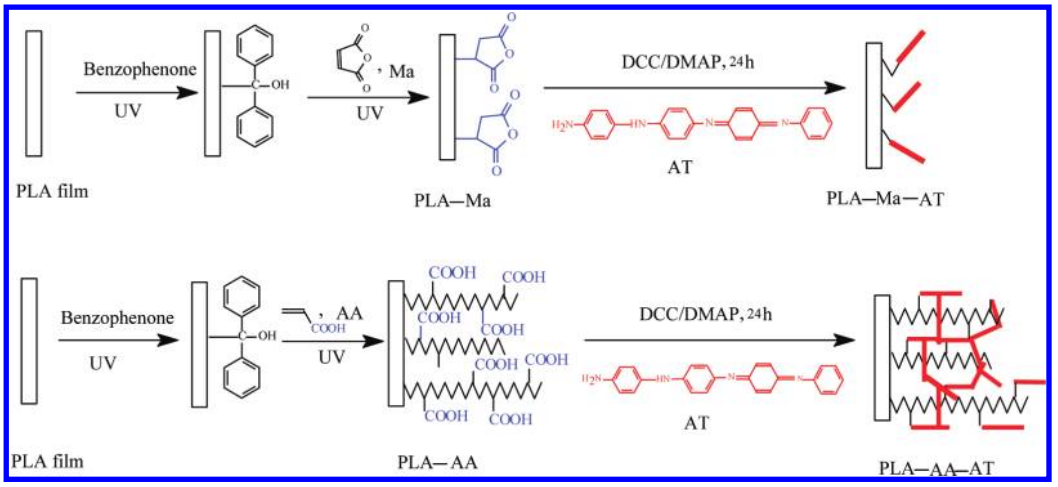

Figure 1. Surface grafting of polylactide (PLA) films with aniline tetramer (AT).

limitation of the conducting polymers used in tissue engineering is their nondegradability. In contrast, aniline oligomers such as aniline trimer, aniline tetramer, and aniline pentamer have a well-defined structure, good biocompatibility, and an electroactivity similar to that of polyaniline, together with specific end groups which offers possibilities for further extensive modification.[27,28] In addition, the aniline oligomers would be consumed by macrophages, and subsequently cleared by the kidney,[29,30] which eliminates the need for a second surgical removal of the materials. Our group have designed and synthesized a series of linear (diblock[31] and triblock[32]), star-shaped,[33] hyperbranched,[34] and cross-linked[35,36] degradable and electrically conducting polymers and hydrogels and porous tubular scaffolds[37] based on PLA, PCL, and aniline oligomers, and we have found that macromolecular architecture is a useful tool to tune the properties of these polymers. All these studies have focused on the bulk properties of the materials.

The goal of the present work is to functionalize the PLA film with aniline oligomer to create a conductive and hydrophilic surface by covalent surface modification. We hypothesize that a moderately hydrophilic PLA surface would have a better interaction with the host tissue and that the electrically conductive PLA surface could be used to induce specific cellular responses to tune and control the formation of new tissue. A covalent modification with AT is preferred rather than noncovalent modification because of its superior environmental stability. First, we introduce maleic anhydride and acrylic acid which contain carboxyl groups to the surface of the PLA film by photografting. Second, we attach the electroactive aniline tetramer to these pendant carboxyl groups by a coupling reaction. The hydrophilic and electroactive surface of PLA films together with the bulk properties of PLA, such as its good mechanical properties, has a great potential in tissue engineering applications.

EXPERIMENTAL SECTION

Materials. Polylactide (PLA) with a molecular weight of 200 000 was bought from Nature Works Co. Ltd. Acrylic acid (AA, Aldrich) was distilled under reduced pressure before use. Maleic anhydride (Ma), *N*-phenyl-1,4-phenylenediamine, ammonium persulfate ($(NH_4)_2S_2O_8$), phenylhydrazine, ammonium hydroxide (NH_4OH), hydrochloric acid (HCl), *N*,*N*′-dicyclohexylcarbodiimide (DCC), 4-(dimethylamino)pyridine (DMAP), ethanol (EtOH), and dimethyl sulfoxide (DMSO, dried with molecular sieve) were all purchased from Aldrich and used without further purification.

Aniline tetramer (AT) was synthesized according to ref 38. ^{1}H NMR (400 MHz, DMSO-d_6): 8.36 (s, 1H), 7.23 (t, 2H), 7.07 (s, 4H), 7.04−6.96 (m, 5H), 6.91−6.82 (m, 2H), 6.83−6.79 (m, 2H), 6.62−6.60 (m, 2H), 5.54 (s, 2H). These data agree with the literature.[38]

Preparation of PLA Films. PLA films were fabricated by a solution-casting method. 1.2 g of PLA was dissolved in 20 mL of $CHCl_3$, and the solution was poured into a silanized Petri dish. The Petri dish was covered and then placed in a horizontal position. $CHCl_3$ was allowed to evaporate at room temperature for 1 week. The PLA film was then peeled from the Petri dish and dried in a vacuum oven. The thickness of the film was determined by a thickness meter (Mitutoyo Corp., Japan) at five different points, and an average value was taken as the film thickness. The PLA film after drying was cut into 2 × 2 cm squares with a thickness of about 108 μm.

Synthesis of PLA-Ma and PLA-AA. PLA films were washed in ethanol and then immersed in a 5% w/w solution of benzophenone in ethanol. The solution was purged with nitrogen for 10 min, and it was then placed under the UV lamp (Osram Ultra-Vitalux 300 W lamp) to activate the PLA film. The distance between the sample and lamp was 50 cm. After irradiation for 20 min, the PLA films were washed many times in ethanol to remove the unbonded benzophenone. The films were finally dried in a vacuum oven for 24 h.

The benzophenone-activated PLA films were soaked in 10% w/w maleic anhydride (Ma) solution in ethanol and purged with nitrogen for 10 min. The mixture was then placed under a UV lamp (Osram Ultra-Vitalux 300 W lamp) to initiate the reaction. After 5 h, the films were taken from the solution and extensively washed with ethanol to remove unreacted maleic anhydride. The sample was finally dried in a vacuum oven for 48 h. The reaction route is shown in Figure 1.

Acrylic acid (AA) was photografted to PLA film by a procedure similar to that used for the preparation of PLA-Ma sample. The samples were coded as PLA-AA2h, PLA-AA3.5 h, and PLA-AA5h, which means that the samples were respectively grafted with AA for 2, 3.5, and 5 h.

Synthesis of PLA-Ma-AT and PLA-AA-AT. PLA-Ma-AT and PLA-AA-AT were prepared by a coupling reaction between the carboxyl group of Ma or AA and amino group of AT with DCC as water condensing agent and DMAP as catalyst. In general, 80 mg of AT, 112 mg of DCC, and 66.5 mg of DMAP were dissolved in a dry DMSO solution; the PLA-Ma or PLA-AA film sample was then put into the mixture, and the vial was sealed. The vial was then put on a mini-shaker with a shaking speed of 50 rpm at room temperature. The reaction was allowed to proceed for 24 h. The PLA films after grafting with AT were washed first with DMSO to remove the unreacted AT and then with an excess of ethanol to remove the DMSO. The PLA-Ma-AT and the PLA-AA-AT were finally dried in a vacuum oven for 24 h. The synthesis pathway is shown in Figure 1.

For comparison, benzophenone-activated PLA film exposed to UV in the absence of maleic anhydride or acrylic acid for 0, 2, 3.5, and 5 h

dx.doi.org/10.1021/ma202508h | *Macromolecules* 2012, 45, 652−659

were prepared in the same way as that of PLA-Ma and PLA-AA samples. The PLA-Ma and PLA-AA samples after incubation in DMSO for 24 h were also prepared as control samples for water contact angle test and scanning electron microscope observations.

Characterization. FT-IR spectra of AT, PLA, PLA-Ma, PLA-Ma-AT, PLA-AA, and PLA-AA-AT were recorded using a Perkin Elmer Spectrum 2000 spectrometer (Perkin-Elmer Instrument, Inc.) equipped with an attenuated total reflectance (ATR) crystal accessory (Golden Gate). Each spectrum was recorded as the average of 16 scans at a resolution of 2 cm^{-1} for wavenumbers between 4000 and 600 cm^{-1} with a correction for atmospheric water and carbon dioxide. The data obtained were evaluated using the Perkin Elmer Instrument v3.02 software.

The wettability of the PLA films before and after grafting was evaluated by determining the contact angle of water using a contact angle and surface tension meter (KSV instruments Ltd.). A drop of Milli-Q water was placed on the surface of the sample, and images of the water drop were recorded by a digital camera. Contact angle data were obtained by analyzing the images with KSV software. The average contact angle of each sample was obtained from five measurements at different points on the samples.

The morphology of the PLA films and modified PLA films mounted on metal stubs was observed using a field emission scanning electron microscope (FE-SEM, S-4800, Hitachi, Japan).

The surface topography of the PLA, PLA-Ma, PLA-Ma-AT, PLA-AA, and PLA-AA-AT was examined with a Nanoscope III atomic force microscope (AFM) (Digital Instrument Inc.) in the contact mode with a scanning area of 5.0 μm. The average roughness of the PLA surface before and after modification was obtained directly from the AFM images.

The UV−vis spectra of AT, PLA-AA-AT and HCl-doped AT, HCl-doped PLA-AA-AT were recorded with a UV−vis spectrophotometer (UV-2401) using 1,4-dioxane as solvent.

A thermogravimetric analysis (TGA) (Mettler) of the PLA and PLA-AA-AT samples was carried out to determine the thermal stability of the polymers. TGA tests were conducted under a nitrogen atmosphere (nitrogen flow rate 50 mL/min) with a heating rate of 10 °C/min from 50 to 800 °C.

The PLA-Ma-AT and PLA-AA-AT samples were cut into 1 × 1 cm squares and immersed in 1 mol/L HCl for 5 min. They were first dried in air and then dried in a vacuum oven for 48 h. The electrical conductivity of these films was determined by the Van Der Pauw four-probe technique (potentiostat, Solartron, SI 1287).

RESULTS AND DISCUSSION

The hydrophobicity and lack of recognition site for cells on the surface are the disadvantages of polyesters such as PLA and PCL for use in tissue engineering. Surface modification and functionalization are useful tools to overcome these drawbacks while maintaining the bulk properties of the polyesters, such as good biocompatibility, good degradability, and good mechanical strength. In this work, a two-step surface functionalization strategy on PLA films is presented to increase the hydrophilicity of the materials and to introduce conductive aniline oligomers onto the PLA surface to regulate the cell behavior in a later stage. The carboxyl groups (−COOH) from maleic anhydride (Ma) and acrylic acid (AA) were first grafted onto PLA film by photografting. These −COOH groups were subsequently covalently coupled with the amino group ($-NH_2$) of a conductive aniline tetramer segment. The synthesis route is shown in Figure 1, and the PLA film after modification was characterized by FT-IR and UV spectrum analysis.

Surface Covalent Grafting of PLA Films with Aniline Tetramer. FT-IR spectra were used to verify the grafting of the PLA films. The FT-IR spectra of PLA, PLA-Ma, and PLA-Ma-AT are shown in Figure 2 as curves a, b, and c, respectively. Pure PLA showed an absorbance peak at 1747 cm^{-1} corresponding to the ester group in the PLA main chain. Maleic anhydride cannot homopolymerize on the PLA surface due to the steric hindrance. Therefore, Ma only forms a monomeric layer on the PLA surface, and a low intensity of the peaks relating to the succinic anhydride groups is expected. There are no peaks corresponding to anhydride functionality appearing between 1830 and 1740 cm^{-1} in curve b. This implies that the anhydride groups are not present on the PLA surface because the anhydride groups are not very stable, and they may hydrolyze during the film grafting and purification with ethanol. A broad C═O peak at 1640 cm^{-1} is present in curve b, indicating that Ma was chemically grafted onto the PLA surface.[3] The peak at 1640 cm^{-1} is weak because only a small amount of Ma was chemically attached to the PLA surface. Compared to curve b, curve c of PLA-Ma-AT showed two new peaks at 1602 and 1507 cm^{-1}, which correspond respectively to the quinoid ring and benzenoid ring in AT. This indicated that AT was grafted onto the Ma through the coupling reaction between the carboxyl group of Ma and the amino group of AT, as shown in Figure 1.

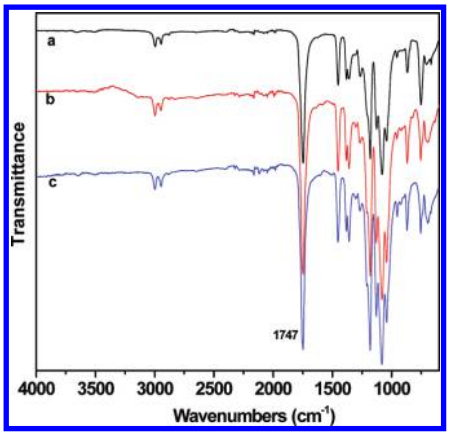

Figure 2. FT-IR spectra of (a) PLA (polylactide), (b) PLA-Ma (polylactide−maleic anhydride), and (c) PLA-Ma-AT (polylactide−maleic anhydride−aniline tetramer).

Compared to the monolayer of carboxyl group from PLA-Ma, the carboxyl polymer brush has a much higher bonding capacity because of the high concentration of carboxyl group at the brush interface. To increase the amount of conductive AT segment on the PLA surface, AA was grafted to PLA films, and PLA-AA samples were synthesized as shown in Figure 1. AA would homopolymerize during the UV irradiation and longer flexible PAA chain was formed, and a large quantity of −COOH groups was introduced onto the PLA film surface. This was confirmed by the FT-IR spectra, as shown in Figure 3. Curves a, b, c, d, and e show the IR spectra of PLA, PLA-AA, AT, PLA-AA2h-AT, and PLA-AA5h-AT, respectively. Compared to curve a, curve b shows that a new peak at 1720 cm^{-1} corresponding to acid group (−COOH) of acrylic acid forms a shoulder peak with that of PLA at 1747 cm^{-1}, indicating that AA was grafted to the PLA film.[17,21] In curve c of AT, the amine group ($-NH_2$) showed two characteristic peaks at 3367 and 3192 cm^{-1}, but in curve d of PLA-AA2h-AT, these two peaks changed into a single broad peak at about 3320 cm^{-1} corresponding to −NH−, indicating that the coupling reaction between the amine group of AT and the carboxyl group of PAA had taken place. In addition, a new peak at 1650 cm^{-1} is assigned to the amide group formed in the coupling reaction of −COOH group of PAA and $-NH_2$ group of AT. The new

dx.doi.org/10.1021/ma202508h | Macromolecules 2012, 45, 652−659

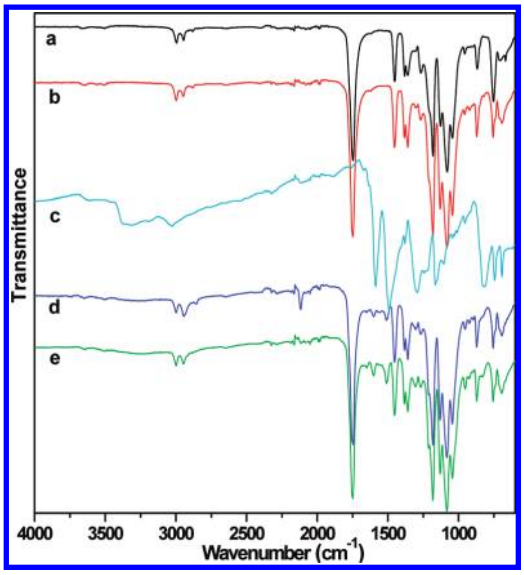

Figure 3. FT-IR spectra of (a) PLA (polylactide), (b) PLA-AA (polylactide–acrylic acid), (c) pure AT (aniline tetramer), (d) PLA-AA2h-AT, and (e) PLA-AA5h-AT.

peaks at 1600 and 1504 cm^{-1} present in curve d, but not in curve b, are attributed to the quinoid ring and benzenoid ring of AT, respectively. The absorption intensities of these peaks are much stronger than those in PLA-Ma-AT, indicating that a larger amount of AT was grafted onto the PLA surface. The peaks at 1650, 1600, and 1510 cm^{-1} in curve e of PLA-AA5h-AT showed a much stronger intensity than in curve d of PLA-AA2h-AT, indicating that the amount of AT grafted onto the PLA surface increased with increasing grafting time of AA to PLA films.

The PLA-AA5h-AT film was dissolved in 1,4-dioxane, and the UV–vis absorption spectrum was recorded as shown in Figure 4. Curve a for AT shows two absorption peaks at 545

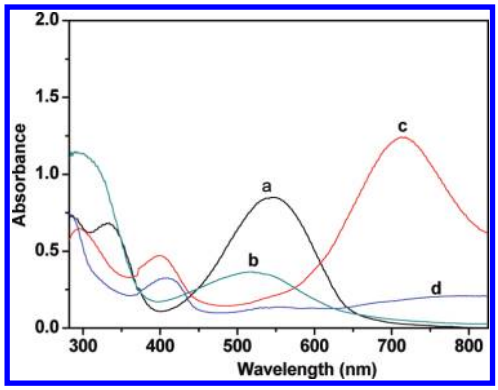

Figure 4. UV–vis spectra of polymers in 1,4-dioxane: (a) AT, (b) PLA-AA5h-AT, (c) HCl-doped AT, and (d) HCl-doped PLA-AA5h-AT.

and 332 nm, corresponding respectively to the characteristic absorption of the excitonic transition from the benzenoid to the quinoid ring and to the $\pi-\pi^*$ transition of the benzenoid ring. In curve b for PLA-AA5h-AT, the absorption of the benzenoid ring shows a hypsochromic shift from 332 to 301 nm, probably because the PAA chains disturb the extent of conjugation between the adjacent phenyl rings in the AT segment.[39] In addition, the quinoid ring absorption underwent a blue shift from 545 to 520 nm, and the ratio of the absorption intensity of the quinoid to the benzenoid ring of PLA-AA5h-AT was less than that of AT. This is because the amide group (−CO−NH−) is an electron-withdrawing group compared to the amino group of AT, and this reduces the electron density of the quinoid ring. These data indicate that the coupling reaction between −COOH and $-NH_2$ had taken place.[33] The HCl-doped AT, as shown in curve c, showed two new absorption peaks at 402 and 712 nm, but the HCl-doped PLA-AA5h-AT showed only one new absorption peak at 402 nm ascribed to the formation of delocalized polarons.[40] This result is consistent with our previous work.[41] These data indicate that the electroactivity of the AT segment was retained after grafting onto the PLA-AA surface.

The amount of AT grafted onto the PLA films was also determined. The AT grafting yield and extent of grafting were calculated by the following equations:

$$\text{grafting yield} = (W_g - W_0)/W_0 \times 100\%$$

$$\text{extent of grafting} = (W_g - W_0)/S$$

where W_g and W_0 represent the weights of the film before and after grafting with AT, and S is the surface area of the PLA film. The results of AT grafting yield and extent of grafting of PLA films are listed in Table 1. The AA grafting yield of PLA-AA2h, PLA-AA3.5h, and PLA-AA5h were 1.0%, 1.6%, and 1.9%, respectively, and they increased with increasing grafting time of AA on PLA surface. The AT grafting yield of PLA-Ma-AT was 2.3%, and the extent of grafting of AT was 380 $\mu g/cm^2$. The PLA-Ma film after grafting with AT was purple in color, indicating that AT was attached to the PLA-Ma surface. The AT grafting yield and extent of grafting of PLA-AA2h-AT were much greater than that of PLA-Ma-AT. For PLA-AA-AT samples, the AT grafting yield and extent of grafting increased with increasing AA grafting time on the PLA film; i.e., the amount of AT grafted onto the PLA-AA surface increased with increasing AA amount on the PLA film. However, the increase was slow after 3.5 h grafting of AA. Therefore, the grafting time of AA was set as 5 h in this work.

Table 1. Extent of Grafting and Grafting Yield of AT on the PLA Films

sample name	extent of grafting ($\mu g/cm^2$)	grafting yield (%)
PLA-Ma-AT	380	2.3
PLA-AA2h-AT	1010	5.7
PLA-AA3.5h-AT	1740	9.9
PLA-AA5h-AT	1850	10.6

Thermal Properties of the Polymers. The AT grafting yield on the PLA surface was also confirmed by TGA, as shown in Figure 5. The PLA showed one degradation stage between 80 and 350 °C in a nitrogen atmosphere. The slight weight loss between 80 and 150 °C may be attributed to a loss of the solvent and moisture entrapped in the polymer. However, the PLA-AA-AT samples showed a two-step degradation process. The first degradation occurred between 50 and 360 °C, which indicates a higher thermal stability than pure PLA, probably due to the better thermal stability of the grafted AT. The second degradation process took place between 360 and 600 °C, and this is attributed to a degradation of the AT segment. The second degradation stage of PLA-AA5h-AT was used to determine the AT content in the PLA film because the PLA

dx.doi.org/10.1021/ma202508h | Macromolecules 2012, 45, 652–659

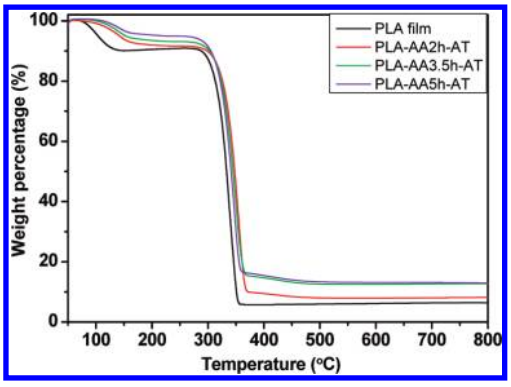

Figure 5. TGA curves of the PLA, PLA-AA2h-AT, PLA-AA3.5h-AT, and PLA-AA5h-AT.

was completely degraded in the first degradation stage. The AT contents determined from the TGA curves agree with the AT grafting yield results shown in Table 1. This further confirmed that the AT segment was successfully grafted onto the PLA-AA surface.

Wettability of the PLA Surfaces after Modification. The surface hydrophilicity, surface charge, surface energy, and surface roughness have great effect on the cell adhesion on the materials.[42−44] Moderate surface hydrophilicity has been shown to be important for cell attachment and cell adhesion.[44,45] The wettability of the PLA surface before and after modification was assessed by determining the contact angle of water, and the results are shown in Figure 6. The contact angle of water on the

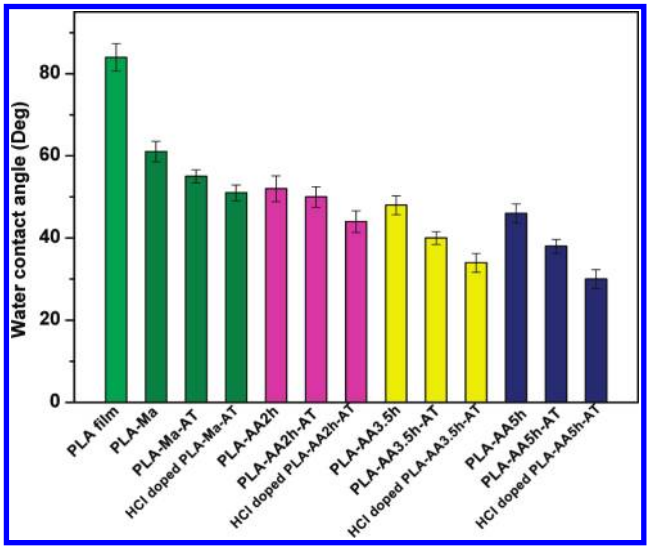

Figure 6. Contact angles of water on the polymer films.

pure PLA surface was about 84°, which is quite hydrophobic. The values of contact angle on the benzophenone activated PLA film exposed to UV in the absence of maleic anhydride or acrylic acid for 0, 2, 3.5, and 5 h were 82°, 81°, 77°, and 76°, respectively. They decreased slightly compared to that of PLA, and these results are consistent with earlier published results.[17] The contact angle of water on PLA-Ma was 61° as a result of the hydrophilic carboxyl group introduced onto the PLA surface. The PLA-AA exhibited a lower contact angle than PLA, and it decreased with increasing grafting time of AA (Figure 6). However, the contact angle was almost stable for PLA-AA3.5 h and PLA-AA5h samples. The contact angles of PLA-Ma, PLA-AA2h, PLA-AA3.5 h, and PLA-AA5h after incubation in DMSO for 24 h were 59°, 56°, 51°, and 46°, respectively. These values were somewhat higher or similar to those of PLA-Ma, PLA-AA2h, PLA-AA3.5 h, and PLA-AA5h, which were 61°, 52°, 48°, and 46°, respectively (Figure 6). The PLA-Ma-AT and PLA-AA-AT sample showed lower contact angle than the corresponding PLA-Ma and PLA-AA samples, probably because the unreacted −COOH groups on the PLA surface doped the AT segment and formed a self-doped polymer.[39,46] The hydrophilicity increased due to the self-doped AT segments. The contact angle of PLA-AA-AT also decreased with increasing AA grafting time because the AT segment has a greater chance to become covalently attached to the larger quantity of −COOH groups. The contact angle of water on the HCl-doped PLA-Ma-AT and PLA-AA-AT was much less than on the corresponding PLA-Ma-AT and PLA-AA-AT because HCl is a strong acid compared to AA and the doped AT form increased sharply.[39,46] The values of the contact angle of water on the (HCl-doped) PLA-Ma-AT and (HCl-doped) PLA-AA-AT were between 58 and 30°, which is much more hydrophilic than pristine PLA, and this will improve the cell attachment on these modified PLA surfaces.[44,45]

Electrical Conductivity of the AT-Modified PLA Films. The electrical conductivity of the PLA films grafted with AT doped with 1 mol/L HCl are listed in Table 2. The

Table 2. Electrical Conductivity of the Films

sample name	conductivity (S/cm)
PLA-Ma-AT	4.36×10^{-8}
PLA-AA2h-AT	1.01×10^{-7}
PLA-AA3.5h-AT	5.57×10^{-7}
PLA-AA5h-AT	6.43×10^{-7}

conductivity of PLA-Ma-AT was about 4.36×10^{-8} S/cm, probably due to the quite low AT grafting yield on the PLA-Ma surface. The conductivity of PLA-AA-AT samples was between 1.01×10^{-7} and 6.43×10^{-7} S/cm, and it increased with increasing AT grafting yield on the PLA surface. This is because the AT segment formed a condensed layer and an intricate conductive network with increasing grafting yield of AT. This conductivity was comparably low because the AT layer on the PLA surface was thin. However, this conductivity value may be sufficient for biomedical applications, since the microcurrent in the human body is quite low.[47] In addition, electroactive polymers with a relatively low conductivity due to the low content of aniline oligomers in the materials can enhance cell adhesion and differentiation without electrical stimulation.[48,49] The AT layer on the PLA surface has direct contact with the host tissue when it is transplanted into human body, and this electroactive layer may improve the cell adhesion and could be used to tune the cellular activity in a later stage. The role of the AT-modified PLA films in adjusting cell functions will be explored in the future.

Morphology of the Films. The morphology of biomaterials is very important for biomedical applications. The morphology of the PLA films before and after photografting was examined by SEM, as shown in Figure 7. The pure PLA film showed a rather flat and smooth surface (Figure 7a). Benzophenone-activated PLA film exposed to UV in the absence of Ma or AA for 0, 2, 3.5, and 5 h also showed a smooth surface (see Figure 1 in the Supporting Information). The surface of Ma-grafted PLA films in Figure 7b is slightly

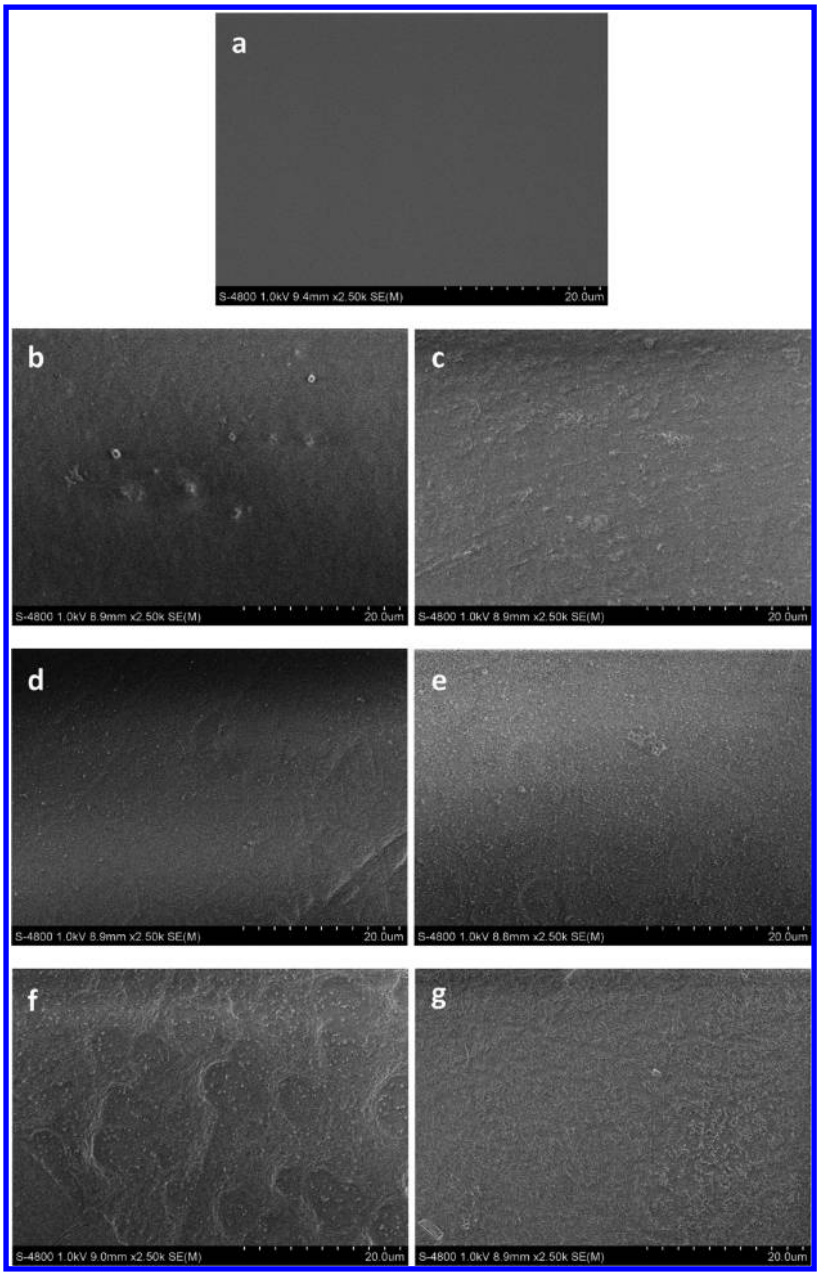

Figure 7. Representative SEM images of the surfaces: (a) PLA, (b) PLA-Ma, (c) PLA-Ma-AT, (d) PLA-AA2h, (e) PLA-AA2h-AT, (f) PLA-AA5h, and (g) PLA-AA5h-AT.

rougher than that of the PLA film. Figure 7d for PLA-AA2h and Figure 7f for PLA-AA5h show that AA segments totally covered the PLA surface. Especially in Figure 7f, the AA segment formed a dense AA layer, and the small round dots are probably attributed to the grafted AA brushes and increase with increasing grafting time of AA compared to Figure 7d. There is no hill appearing on the surface of PLA-Ma and PLA-AA after incubation in DMSO for 24 h (see Figure 2 in the Supporting Information). PLA-Ma-AT (Figure 7c) exhibited a rougher morphology than PLA-Ma in Figure 7b, and some small hills appeared. The PLA-AA2h-AT and PLA-AA5h-AT images in Figure 7e,g show that a condensed AT layer was formed on the PLA-AA surface. Some small dots on the PLA-AA-AT surface probably correspond to the aggregates of AT segments after grafting on the AA brushed, since AT segment would gather together due to their strong interaction between the AT moiety. The AT layer could be doped by acid and provided a conductive surface. These surface changes were also confirmed by AFM observations. For example, the AFM image in Figure 8a for PLA film showed a smooth surface with a roughness of 3 nm. The PLA-Ma (Figure 8b) and PLA-Ma-AT (Figure 8c) images both showed a slightly rougher surface with a roughness of 8 and 17 nm, respectively. These roughness increases indicate that the Ma was successfully grafted onto PLA films and that AT was subsequently attached onto the PLA-Ma. AFM images of PLA-AA5h and PLA-AA5h-AT are shown in Figure 8d,e. The surface of PLA-AA5h with a roughness of 32 nm is much rougher than that of PLA-Ma, indicating that the grafting yield of AA increased dramatically compared to that of PLA-Ma. The roughness of PLA-AA5h-AT is 26 nm, which is higher than that of PLA-Ma-AT but slightly lower than that of PLA-AA5h. This may be because the strong interactions between the

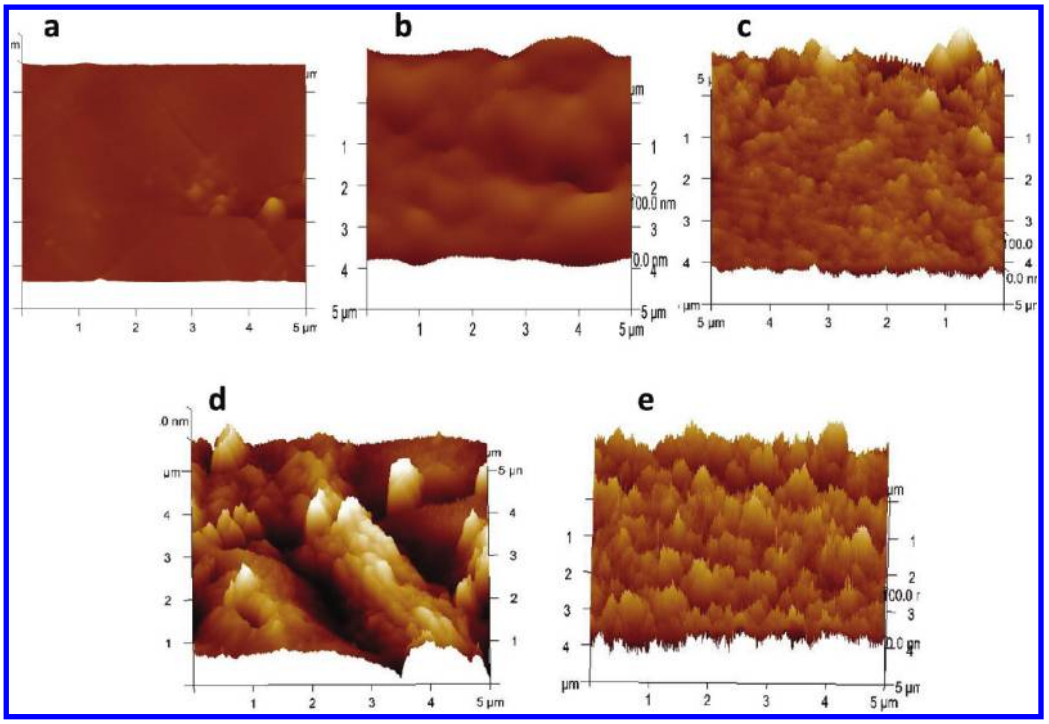

Figure 8. Representative AFM images of PLA surface before and after modification: (a) pristine PLA film, (b) PLA-Ma, (c) PLA-Ma-AT, (d) PLA-AA5h, and (e) PLA-AA5h-AT.

AT segment grafted on PAA chain make the molecular brushes entangle with each other, and a denser surface with a lower roughness is consequently formed. These results are consistent with the SEM images in Figure 7 and FT-IR spectra in Figure 3 and AT grafting yield data in Table 1.

We have demonstrated a versatile method for the covalent surface functionalization of polyester films to create a conducting hydrophilic surface. Different polyesters such as polycaprolactone, poly(1,5-dioxepan-2-one), poly(trimethylene carbonate), and their copolymers with different degradation, mechanical, and thermal properties can be used as substrate films. In addition, different aniline oligomers such as aniline trimer, aniline tetramer, and aniline pentamer, etc., with different electrical conductivities can be employed for coupling to the polyester surface. Therefore, this versatile technique will lead to a library of materials exhibiting a tunable conductivity and hydrophilic surface through the choice of the suitable substrates and aniline oligomers. This could meet the requirement for a particular biomedical application.

CONCLUSIONS

An electroactive and hydrophilic polylactide (PLA) surface was successfully developed by the photografting of acrylic acid (AA) and maleic anhydride (Ma) onto PLA film and subsequent coupling with conductive aniline tetramer (AT). The contact angle of water on the PLA film after grafting and coupling reaction with AT decreased sharply, indicating that a more hydrophilic surface was obtained. The UV grafting and coupling reaction between the carboxyl group of AA (or Ma) and the amino group of AT was confirmed by FT-IR, UV, TGA, and grafting yield determination. The grafting yield of AT on the PLA surface increased with increasing time of grafting of AA onto the PLA films. The conductivity of the PLA surface after coupling with AT is in the range of a semiconductor, and the conductivity increased with the increasing AT grafting yield on the PLA films. The roughness of the PLA surfaces after modification increased dramatically, as demonstrated by SEM and AFM observations. These PLA films with a moderate hydrophilic and electroactive surface will find application in tissue regeneration.

ASSOCIATED CONTENT

Supporting Information

SEM images of benzophenone activated PLA film exposed to UV in the absence of Ma or AA for 0, 2, 3.5, and 5 h and SEM images of PLA-Ma and PLA-AA samples after incubation in DMSO for 24 h. This material is available free of charge via the Internet at http://pubs.acs.org.

AUTHOR INFORMATION

Corresponding Author

*Tel +46-8-790 8274; Fax +46-8-20 84 77; e-mail aila@polymer.kth.se.

ACKNOWLEDGMENTS

The authors are grateful to the China Scholarship Council (CSC) and The Royal Institute of Technology (KTH) for financial support for this work. We thank Robertus Wahyu Nayan Nugroho for AFM measurement.

REFERENCES

(1) Elbert, D. L.; Hubbell, J. A. *Annu. Rev. Mater. Sci.* **1996**, *26*, 365–394.
(2) Goddard, J. M.; Hotchkiss, J. H. *Prog. Polym. Sci.* **2007**, *32*, 698–725.
(3) Edlund, U.; Kallrot, M.; Albertsson, A. C. *J. Am. Chem. Soc.* **2005**, *127*, 8865–8871.
(4) Hubbell, J. A. *Bio-Technology* **1995**, *13*, 565–576.
(5) Nair, L. S.; Laurencin, C. T. *Prog. Polym. Sci.* **2007**, *32*, 762–798.
(6) Albertsson, A. C.; Varma, I. K. *Biomacromolecules* **2003**, *4*, 1466–1486.

(7) Jiao, Y. P.; Cui, F. Z. *Biomed. Mater.* **2007**, *2*, R24−R37.
(8) Rasal, R. M.; Janorkar, A. V.; Hirt, D. E. *Prog. Polym. Sci.* **2010**, *35*, 338−356.
(9) Xu, F. J.; Yang, X. C.; Li, C. Y.; Yang, W. T. *Macromolecules* **2011**, *44*, 2371−2377.
(10) Oh, J. K. *Soft Matter* **2011**, *7*, 5096−5108.
(11) Wan, Y. Q.; Chen, W. N.; Yang, J.; Bei, J. Z.; Wang, S. G. *Biomaterials* **2003**, *24*, 2195−2203.
(12) Deng, C.; Chen, X. S.; Sun, J.; Lu, T. C.; Wang, W. S.; Jing, X. B. *J. Polym. Sci., Part A: Polym. Chem.* **2007**, *45*, 3218−3230.
(13) Spasova, M.; Mespouille, L.; Coulembier, O.; Paneva, D.; Manolova, N.; Rashkov, I.; et al. *Biomacromolecules* **2009**, *10*, 1217−1223.
(14) Cai, Q.; Yang, J. A.; Bei, J. Z.; Wang, S. G. *Biomaterials* **2002**, *23*, 4483−4492.
(15) Wan, Y.; Wu, H.; Yu, A. X.; Wen, D. J. *Biomacromolecules* **2006**, *7*, 1362−1372.
(16) Deng, J. P.; Wang, L. F.; Liu, L. Y.; Yang, W. T. *Prog. Polym. Sci.* **2009**, *34*, 156−193.
(17) Janorkar, A. V.; Metters, A. T.; Hirt, D. E. *Macromolecules* **2004**, *37*, 9151−9159.
(18) Rasal, R. M.; Bohannon, B. G.; Hirt, D. E. *J. Biomed. Mater. Res., Part B* **2008**, *85B*, 564−572.
(19) Janorkar, A. V.; Proulx, S. E.; Metters, A. T.; Hirt, D. E. *J. Polym. Sci., Part A: Polym. Chem.* **2006**, *44*, 6534−6543.
(20) Hoglund, A.; Hakkarainen, M.; Edlund, U.; Albertsson, A. C. *Langmuir* **2010**, *26*, 378−383.
(21) Kallrot, M.; Edlund, U.; Albertsson, A. C. *Biomacromolecules* **2007**, *8*, 2492−2496.
(22) Wong, J. Y.; Langer, R.; Ingber, D. E. *Proc. Natl. Acad. Sci. U. S. A.* **1994**, *91*, 3201−3204.
(23) Shi, G. X.; Zhang, Z.; Rouabhia, M. *Biomaterials* **2008**, *29*, 3792−3798.
(24) Gumus, A.; Califano, J. P.; Wan, A. M. D.; Huynh, J.; Reinhart-King, C. A.; Malliaras, G. G. *Soft Matter* **2010**, *6*, 5138−5142.
(25) Lee, J. Y.; Bashur, C. A.; Goldstein, A. S.; Schmidt, C. E. *Biomaterials* **2009**, *30*, 4325−4335.
(26) Xie, J. W.; MacEwan, M. R.; Willerth, S. M.; Li, X. R.; Moran, D. W.; Sakiyama-Elbert, S. E.; et al. *Adv. Funct. Mater.* **2009**, *19*, 2312−2318.
(27) Wei, Z. X.; Faul, C. F. J. *Macromol. Rapid Commun.* **2008**, *29*, 280−292.
(28) Udeh, C. U.; Fey, N.; Faul, C. F. J. *J. Mater. Chem.* **2011**, *21*, 18137−18153.
(29) Rivers, T. J.; Hudson, T. W.; Schmidt, C. E. *Adv. Funct. Mater.* **2002**, *12*, 33−37.
(30) Green, T. R.; Fisher, J.; Matthews, J. B.; Stone, M. H.; Ingham, E. *J. Biomed. Mater. Res.* **2000**, *53*, 490−497.
(31) Guo, B. L.; Finne-Wistrand, A.; Albertsson, A. C. *Macromolecules* **2011**, *44*, 5227−5236.
(32) Guo, B. L.; Finne-Wistrand, A.; Albertsson, A. C. *Chem. Mater.* **2011**, *23*, 4045−4055.
(33) Guo, B. L.; Finne-Wistrand, A.; Albertsson, A. C. *Biomacromolecules* **2010**, *11*, 855−863.
(34) Guo, B. L.; Finne-Wistrand, A.; Albertsson, A. C. *Macromolecules* **2010**, *43*, 4472−4480.
(35) Guo, B. L.; Finne-Wistrand, A.; Albertsson, A. C. *J. Polym. Sci., Part A: Polym. Chem.* **2011**, *49*, 2097−2105.
(36) Guo, B. L.; Finne-Wistrand, A.; Albertsson, A. C. *Biomacromolecules* **2011**, *12*, 2601−2609.
(37) Guo, B. L.; Sun, Y.; Finne-Wistrand, A.; Mustafa, K.; Albertsson, A. C. *Acta Biomater.* **2012**, *8*, 144−153.
(38) Rozalska, I.; Kulyk, P.; Kulszewicz-Bajer, I. *New J. Chem.* **2004**, *28*, 1235−1243.
(39) Chan, H. S. O.; Ng, S. C.; Sim, W. S.; Tan, K. L.; Tan, B. T. G. *Macromolecules* **1992**, *25*, 6029−6034.
(40) Xia, Y. N.; Wiesinger, J. M.; Macdiarmid, A. G.; Epstein, A. J. *Chem. Mater.* **1995**, *7*, 443−445.
(41) Guo, B. L.; Finne-Wistrand, A.; Albertsson, A. C. *Chem. Mater.* **2011**, *23*, 1254−1262.
(42) Reuveny, S.; Mizrahi, A.; Kotler, M.; Freeman, A. *Biotechnol. Bioeng.* **1983**, *25*, 469−480.
(43) Denbraber, E. T.; Deruijter, J. E.; Smits, H. T. J.; Ginsel, L. A.; Vonrecum, A. F.; Jansen, J. A. *J. Biomed. Mater. Res.* **1995**, *29*, 511−518.
(44) Lampin, M.; WarocquierClerout, R.; Legris, C.; Degrange, M.; SigotLuizard, M. F. *J. Biomed. Mater. Res.* **1997**, *36*, 99−108.
(45) Vanwachem, P. B.; Hogt, A. H.; Beugeling, T.; Feijen, J.; Bantjes, A.; Detmers, J. P.; et al. *Biomaterials* **1987**, *8*, 323−328.
(46) Kim, S. C.; Whitten, J.; Kumar, J.; Bruno, F. F.; Samuelson, L. A. *Macromol. Res.* **2009**, *17*, 631−637.
(47) Niple, J. C.; Daigle, J. P.; Zaffanella, L. E.; Sullivan, T.; Kavet, R. *Bioelectromagnetics* **2004**, *25*, 369−373.
(48) Hu, J.; Huang, L. H.; Zhuang, X. L.; Zhang, P. B.; Lang, L.; Chen, X. S.; et al. *Biomacromolecules* **2008**, *9*, 2637−2644.
(49) Liu, Y. D.; Hu, J.; Zhuang, X. L.; Zhang, P. B. A.; Chen, X. S.; Wei, Y.; et al. *Macromol. Biosci.* **2011**, *11*, 806−813.